Fermi National Accelerator Laboratory

FERMILAB-Conf-99/087-E
CDF and D0

Dijet Results from CDF and D0

Takashi Asakawa
For the CDF and D0 Collaborations

University of Tsukuba
Tsukuba, Ibaraki 305, Japan

Fermi National Accelerator Laboratory
P.O. Box 500, Batavia, Illinois 60510

April 1999

Published Proceedings of the *13th Topical Conference on Hadron Collider Physics*, Mumbai, India, January 14-20, 1999

CDF/PUB/QCD/PUBLIC/4937
Version 2
March 30, 1999

Dijet Results from CDF and DØ

Takashi Asakawa
University of Tsukuba
Tsukuba, Ibaraki 305, Japan

for the
CDF and DØ Collaborations

13th Topical Conference on Hadron Collider Physics
Mumbai, India
January 14-20, 1999

DIJET RESULTS FROM CDF AND DØ

TAKASHI ASAKAWA
Institute of Physics, University of Tsukuba,
Tsukuba, Ibaraki, 305, Japan
for the
CDF and DØ Collaborations

Recent results on the measurement of the dijet inclusive differential cross section and the dijet mass distribution made by the CDF and DØ collaborations are presented. The analyses are based on large statistics of data obtained from the 94-95 Tevatron collider run at Fermilab. The measured spectra are compared to QCD calculations using different parton distribution functions. The CDF and DØ dijet angular distributions are also presented to be compared to QCD calculations.

1 Introduction

In QCD a hard scattering process between hadrons is the result of an interaction between the constituents of the incoming hadrons: quarks and gluons. In dijet production at Tevatron an incoming parton from a proton scatters off an incoming parton from an antiproton, and the resulting two high-transverse-momentum partons are observed as "*jets*". Next-Leading Order (NLO) QCD calculations are available[1,2] which predict the dijet production over a wide range of the jet transverse energy. Measurements of dijet production cross section provide a test of NLO QCD calculations and help us constrain the parton distribution functions (PDF) at high x and high Q^2.

An orthogonal approach to the dijet production is the measurement of the angular distribution. In the parton-parton center-of-mass system, the angular distribution is sensitive to the form of the $2 \to 2$ matrix elements. The analysis of the dijet angular distribution enables us to study the properties of parton-parton scattering without a strong dependence on the choice of the PDF.

2 The Inclusive Dijet Differential Cross Section

The CDF analysis is based on dijet data (87 pb^{-1}) taken in the 94-95 collider run (Run IB). The data were collected using inclusive E_T triggers with online E_T thresholds of 20, 50, 70, and 100 GeV. Jets are identified by a cone clustering algorithm with cone radius $\mathcal{R}= \sqrt{(\Delta\phi)^2 + (\Delta\eta)^2} = 0.7$, and events with at least two reconstructed jets are selected. The "*trigger jet*" is required to satisfy $E_T > 40$ GeV and to sit in the well calibrated central region of the calorimeter, $0.1 < |\eta_1| < 0.7$. The *trigger jet* is used to measure E_T of the event. The "*probe jet*" is required to satisfy $E_T > 10$ GeV and to sit in one of four pseudorapidity bins: $0.1 < |\eta_2| < 0.7$, $0.7 < |\eta_2| < 1.4$, $1.4 < |\eta_2| < 2.1$, or $2.1 < |\eta_2| < 3.0$. No restriction on any additional jets is applied. In the case that the *probe jet* also satisfies the *trigger jet* selection requirements, both combinations contribute to the distribution. The measured jet energies are corrected for detector resolution using the same procedure used in the measurement of the inclusive jet cross section[3].

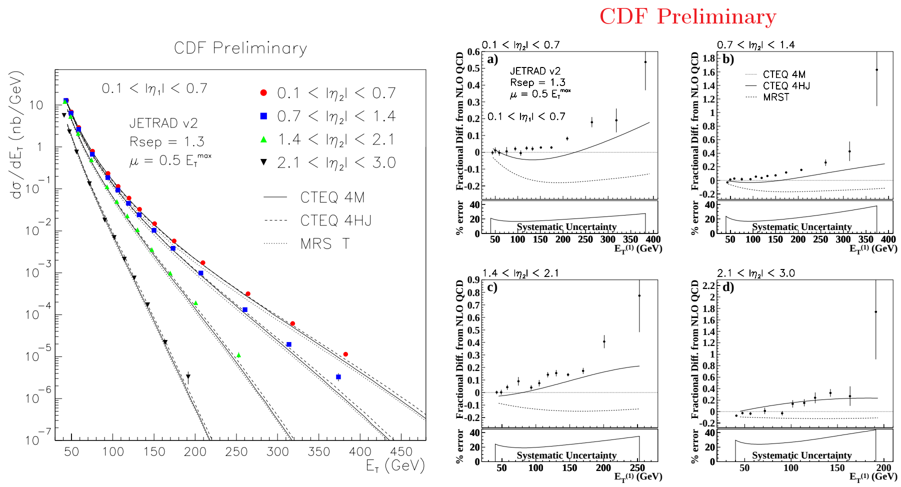

Figure 1. The CDF dijet differential cross section compared to NLO QCD using different PDFs (left) and the fractional difference from the predictions using CTEQ4M (right).

The cross section is measured as a function of E_T of the *trigger jet*. The results are compared to NLO QCD calculations of JETRAD[1] using different PDFs in Figure 1(left). The four separate distributions correspond to the four different pseudorapidity bins of the *probe jet*. A detailed comparison is made in Figure 1(right); the relative difference of data from NLO QCD for CTEQ4M[4], $\mathcal{R}_{\rm sep} = 1.3$, and $\mu = 0.5E_T^{\rm max}$. In all the η_2 bins the observed data are in good agreement to CTEQ4M at $E_T < 100$ GeV and are larger than the prediction at higher E_T. We should note that the systematic uncertainty ranging from 20-40% is highly correlated. Predictions using other PDFs (CTEQ4HJ[4], MRST[5]) are also shown in the same figure compared to the default prediction. These distributions are seen to be sensitive to the choice of PDFs.

The E_T and pseudorapidities of the leading jets are related to the momentum fractions (x) of the partons involved in the interaction. In leading order the relation is

$$x_1 = \frac{E_T}{\sqrt{s}}(e^{\eta_1} + e^{\eta_2}); \quad x_2 = \frac{E_T}{\sqrt{s}}(e^{-\eta_1} + e^{-\eta_2}). \tag{1}$$

For fixed E_T and η_1, different momentum fractions can be selected by requiring that the *probe jet* lie in different η intervals. For a two-body process one intuitive choice for Q^2 for the event is

$$Q^2 \sim -\hat{t} = 2e_t^2 \cosh^2 \eta^\star (1 - \tanh \eta^\star) \tag{2}$$

where $\eta^\star = (\eta_1 - \eta_2)/2$. The observed data converted from (E_T, η_2) bins to ($x_{\rm max}$, $\hat{t}$) bins are shown in Figure 2(left). Note that we define $x_{\rm max}$ as the maximum of x_1 and x_2.

The DØ analysis uses 92 pb^{-1} of data taken in Run IB. The analysis is started by selecting events with at least two reconstructed jets which sit in any of the following four pseudorapidity bins: $0.0 < |\eta| < 0.5$, $0.5 < |\eta| < 1.0$, $1.0 < |\eta| < 1.5$,

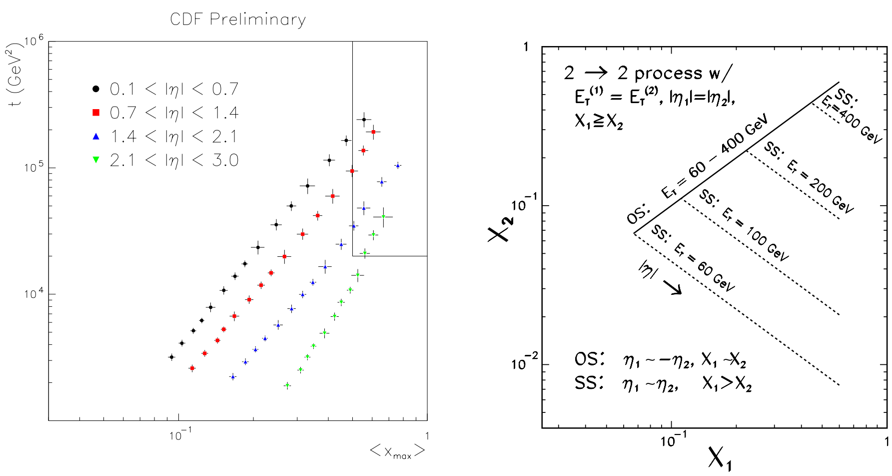

Figure 2. The kinematic region probed by the CDF and DØ measurements of the dijet differential cross section; left: the $x_{\max}$ and $\hat{t}$ region probed by the CDF measurement and right: the x_1 and x_2 region covered by the DØ measurement.

and $1.5 < |\eta| < 2.0$. Events in each η bin are then divided into two subsamples according to their event topology; events with 2 jets on the Opposite Side of the detector (OS) and events with 2 jets on the Same Side of the detector (SS). Since E_T's of both jets are measured, events are always double counted.

The results are shown in Figure 3(a)-(c). The observed data are compared to NLO QCD calculations using $\mu_f = \mu_r = 0.5 \times E_{\max}$ (where $E_{\max}$ is the maximum of E_1 and E_2) and three different PDFs: (a) CTEQ3M[6], (b) CTEQ4M, and (c) MRST. The observed spectra agree to NLO QCD using CTEQ3M and CTEQ4M and are somewhat higher than the prediction using MRST.

In SS events ($\eta_1 \sim \eta_2$), the momentum fractions of the two partons are unbalanced: $x_1 >> x_2$ or $x_1 <<< x_2$, while in OS events ($\eta_1 \sim -\eta_2$), they are balanced: $x_1 \sim x_2$. This is shown in Figure 2(right) for different jet E_T's. The DØ measurement probes the x region down to .01.

The dijet differential cross sections measured by CDF and DØ show reasonable agreement in shape to theoretical predictions with recent parton distribution functions within experimental uncertainties. These measurements cover a wide range of the x–Q^2 plane and the x_1–x_2 plane and can be used to determine further improved PDFs.

3 The Inclusive Dijet Mass Distribution

Both DØ and CDF have measured the dijet differential cross section, $d^3\sigma/dM_{jj}d\eta_1 d\eta_2$, as a function of the dijet mass. The DØ analysis[7] based on 92 pb^{-1} of data collected in Run IB uses events with at least two jets in central, $|\eta| < 1$. The dijet mass is calculated assuming massless jets:

$$M_{jj}^2 = 2E_T^{(1)}E_T^{(2)}(\cosh(\Delta\eta) - \cos(\Delta\phi)) \tag{3}$$

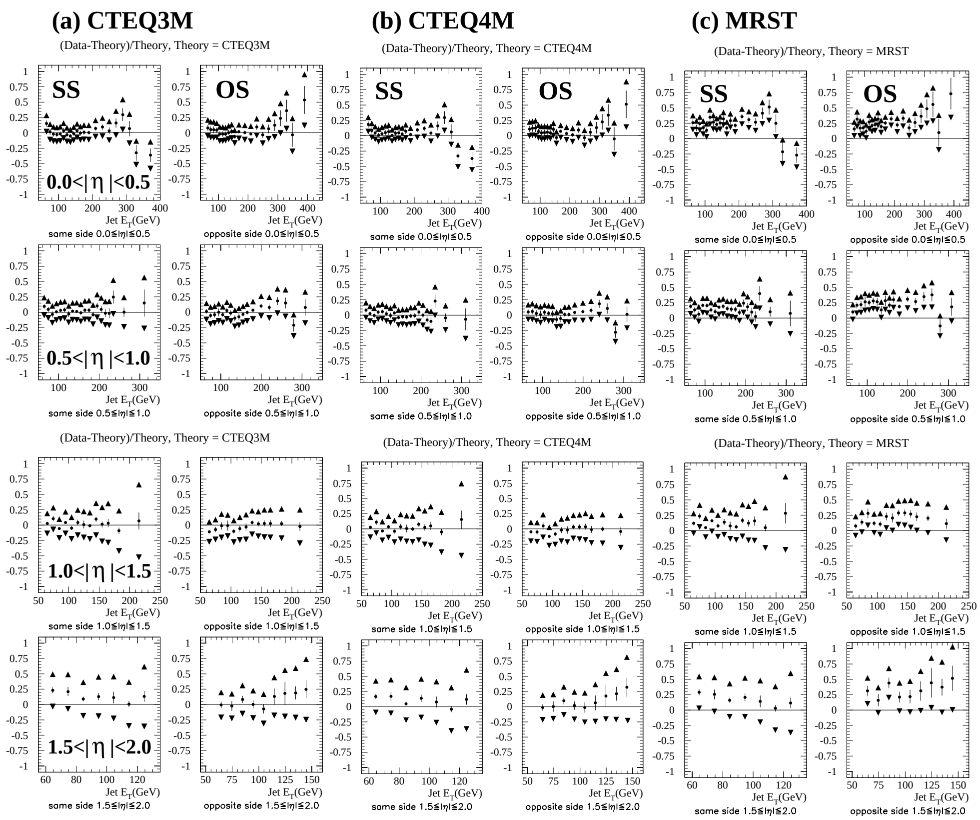

Figure 3. The fractional difference of the DØ dijet differential cross section from NLO QCD using PDFs of (a)CTEQ3M, (b)CTEQ4M, and (c)MRST. The renormalization scale and the factorization scales are chosen to be the maximum of E_1 and E_2.

The DØ dijet mass spectrum is compared to the NLO QCD predictions calculated by JETRAD with CTEQ3M and $\mu = 0.5E_T^{\max}$ in Figure 4(left). A detailed comparison is shown in Figure 4(right) for different choices of PDFs and scales. Table 1 summarizes the χ^2 values resulting from a fit of theory to the data for various choices of the PDFs and the scales. Note that the correlations are taken into account in calculating the χ^2's. From the χ^2 analysis one can conclude that all the choices provide a reasonable description of the observed data.

The CDF analysis based on 87 pb^{-1} of data taken in Run IB uses events with at least two jets with $|\eta| < 2$. We further require dijet events to satisfy $|\cos\theta^\star| < 2/3$, where $\cos\theta^\star = \tanh\eta^\star$. The dijet invariant mass includes the mass of each jet and is calculated from the standard four vectors:

$$M_{jj} = \sqrt{(E_1 + E_2)^2 - (\vec{p}_1 + \vec{p}_2)^2} \tag{4}$$

Since the kinematic ranges are different for the CDF and the DØ measurements, the fractional difference from NLO QCD (CTEQ4M, $\mu = 0.5E_T^{\max}$ are used) is made for both results in Figure 5. There is excellent agreement in the shape of the distributions measured by the two experiments.

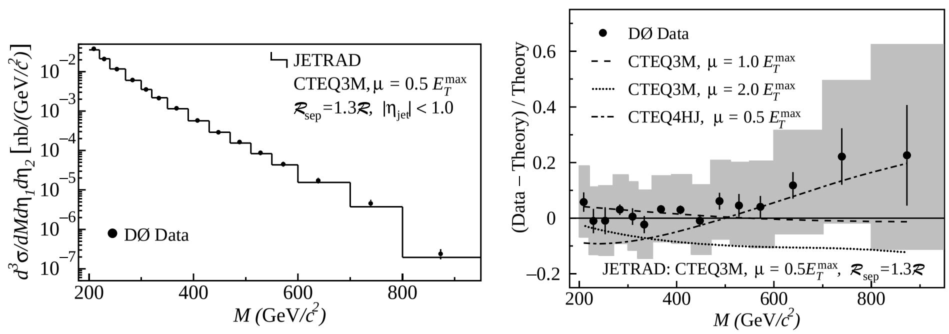

Figure 4. The DØ dijet mass distribution compared to NLO QCD using CTEQ3M (left) and the fractional difference from the predictions using different PDFs (right).

Table 1. χ^2 comparison of the DØ dijet mass data to predictions with different PDFs and scales.

PDF	renorm. scale	χ^2 (15 dof)	Prob.(χ^2)
CTEQ3M	$0.25E_T^{max}$	12.2	0.66
CTEQ3M	$0.50E_T^{max}$	5.0	0.99
CTEQ3M	$0.75E_T^{max}$	5.3	0.99
CTEQ3M	$1.00E_T^{max}$	5.4	0.99
CTEQ3M	$2.00E_T^{max}$	4.2	1.00
CTEQ4M	$0.50E_T^{max}$	4.9	0.99
CTEQ4HJ	$0.50E_T^{max}$	5.0	0.99
MRS(A)′[8]	$0.50E_T^{max}$	6.3	0.97

4 The Inclusive Dijet Angular Distribution

The angular distributions are fairly insensitive to the parton distribution in incoming hadrons. The measurement of the dijet scattering angle in the center-of-mass system provides a fundamental test of QCD and is a sensitive probe of new physics. In both the CDF and DØ analyses the angular variable is defined as

$$\chi \equiv \hat{u}/\hat{t} = \frac{1 + |\cos\theta^\star|}{1 - |\cos\theta^\star|} \simeq e^{|\eta_1 - \eta_2|} \tag{5}$$

where $\theta^\star$ is the scattering angle in the center-of-mass system. Note that $dN/d\chi$ is independent of χ for the Rutherford scattering. The CDF and DØ dijet angular distributions are made for different dijet mass bins and compared to QCD predictions[9,10] in Figure 6. The results from both the experiments are consistent to the NLO QCD predictions. Note the quark compositeness limits obtained from the dijet angular distributions are presented in these proceedings[11].

5 Conclusions

The Tevatron dijet data enable us to probe the high x and high Q^2 region. The dijet differential cross section can be used as an input to global QCD fits. The dijet

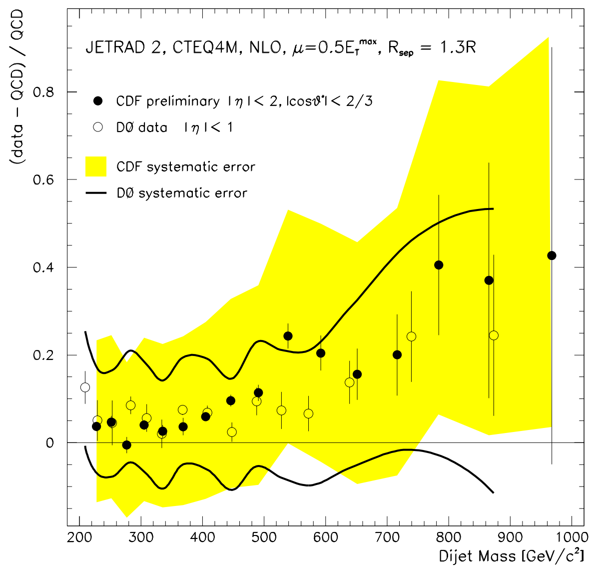

Figure 5. Comparison of the dijet mass distributions from CDF and DØ with theory predictions calculated by JETRAD with CTEQ4M.

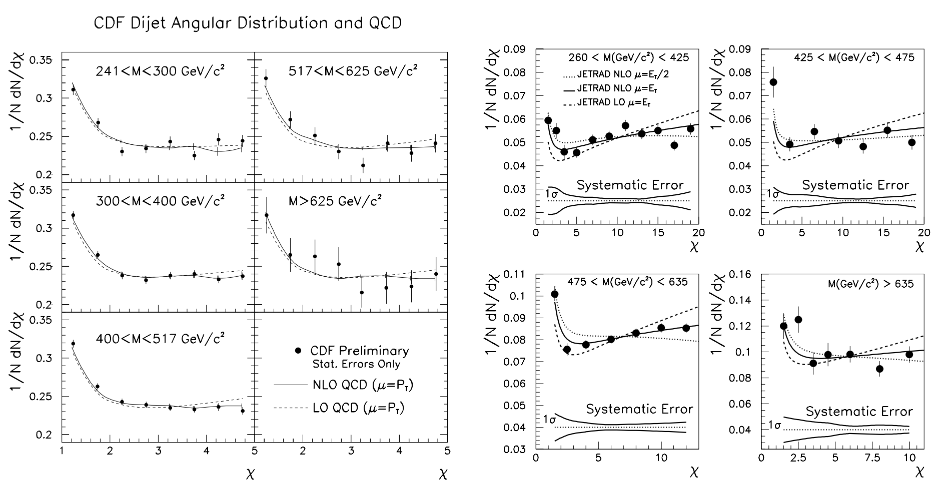

Figure 6. The CDF dijet angular distributions (left) and the DØ angular distributions (right).

differential cross sections measured by CDF and DØ are compared to NLO QCD calculations using different PDFs. The DØ results are in good agreement to NLO QCD using CTEQ3M or CTEQ4M and are somewhat larger than the prediction using MRST. The CDF data are well described by NLO QCD using CTEQ4M at $E_T < 100$ GeV and are larger than the prediction at higher E_T. These distributions are seen to be sensitive to the choice of PDFs.

The NLO QCD predictions give a reasonable description of the DØ and CDF dijet mass distributions. For given the different kinematic regions, the shapes of the DØ and CDF spectra are in excellent agreement.

The dijet angular distributions from CDF and DØ are consistent to NLO QCD. No evidence that might indicate new phenomena was observed.

Acknowledgments

I am indebted to members of the CDF and DØ collaborations for figures presented in this paper and discussions of their data.

References

1. W.T. Giele *et al.*, Nucl. Phys. B **403**, 633(1993).
2. S. Ellis *et al.*, Phys. Rev. Lett. **64**, 2121(1990).
   F. Aversa *et al.*, Nucl. Phys. B **327**, 105(1989).
3. F. Abe *et al.*, CDF Collab., Phys. Rev. Lett. **77**, 438(1996).
4. H.L. Lai *et al.*, CTEQ Collab., Phys. Rev. D **55**, 1280(1997).
5. A.D. Martin, R.G. Roberts, W.J. Stirling, and R.S. Thorne, Eur. Phys. J. C **4**, 463(1998).
6. H.L. Lai *et al.*, CTEQ Collab., Phys. Rev. D **51**, 4763(1995).
7. B. Abbott *et al.*, DØ Collab., Phys. Rev. Lett. **82**, 2457(1999).
8. A.D. Martin, R.G. Roberts, and W.J. Stirling, Phys. Lett. B **354**, 155(1995).
9. F. Abe *et al.*, CDF Collab., Phys. Rev. Lett. **77**, 5336(1996).
   Erratum-ibid. **78**, 4307(1997).
10. B. Abbott *et al.*, DØ Collab., Phys. Rev. Lett. **80**, 666(1998).
11. I.A. Bertram, "Search for Quark Compositeness at the Tevatron", These proceedings.